Manufacturing High-Strength HA-Ti Surface Composites by Friction Stir Processing with Different Filler Mixtures

A. Shahbaz[1], M. Abbasi[1,*], H. Sabet[1]

[1]Department of Materials Engineering, Karaj Branch, Islamic Azad University, Karaj, Iran.
Received: 18 September 2023 - Accepted: 10 May 2024

Abstract

In recent years, a wide range of studies have focused on the surface modification of titanium, especially in terms of its biomedical applications. However, comparatively less researches have been conducted on the fabrication of titanium surface composites in bulk form. The primary objective of this investigation is to successfully produce hydroxyapatite (HA)-Ti surface composites with a homogenous dispersion of nano hydroxyapatite particles through friction stir processing (FSP). The secondary aim is to investigate the effect of FSP parameters, specifically filler mixture, on the microstructure and mechanical properties of the composites. Two different mixtures of HA and FSP parameters, traverse speeds of 30 and 45 mm min^{-1}, rotational speed of 1200 rpm, and a conical tool shape, were used. It was found that the samples obtained by a filler mixture of HA-polyvinyl alcohol (PVA) showed better dispersion of HA in the Ti base, as well as higher tensile strength. Also, a 30 mm min^{-1} traverse speed led to higher strength in both filler mixtures. Therefore, the sample produced by a traverse speed of 30 mm min^{-1} and HA/PVA filler mixture was selected as the optimum sample.

Keywords: Friction Stir Processing, Titanium, Filler Mixture, Hydroxyapatite, Mechanical Properties.

1. Introduction

Surface composites have garnered significant attention in recent years, primarily due to their modified characteristics across various aspects, including enhanced wear resistance. Friction stir processing (FSP) stands out as one of the most effective techniques for synthesizing both surface and bulk composites. The process involves severe plastic deformation, leading to the formation of ultrafine-grained zones. Notably, the FSP process allows for the improvement of surface layer characteristics while keeping the bulk of the sample unchanged [1, 2].Titanium and its alloys have become subjects of extensive research in the realm of metallic biomaterials and orthopedic implants. This is primarily attributed to their favorable biocompatibility, commendable mechanical properties, and remarkable corrosion resistance [3]. In the pursuit of ideal implants, a crucial criterion is the establishment of sufficient adhesion to human tissues, a key factor in preventing implant failure [4].Numerous studies have delved into the exploration of nanocomposites with titanium as the matrix, incorporating various reinforcing powders to predominantly enhance sample hardness and wear resistance. Notable examples include Al2O3[5, 6], SiC[7], TiN [8, 9], TiC[10], and TiO2[11], which have been extensively investigated as reinforcements in prior studies. Conversely, the biocompatibility of titanium alloys emerges as a pivotal aspect, surpassing the mere improvement of mechanical properties in certain cases.

[*]Corresponding author
Email address: mabbasi@kiau.ac.ir

In another study[12], carbon nanotubes (CNTs) were employed as reinforcing material for the titanium matrix through the Friction Stir Processing (FSP) technique. The findings revealed that an increase in the number of passes led to higher strength and hardness of the samples. This phenomenon was attributed to the improved distribution of CNTs within recrystallized grains.
Farnoush et al.[13] conducted a study on the Ti-HA surface composite, employing a combination of FSP and electro-deposition. Their findings revealed that dynamic recrystallization (DRX) during the FSP process led to grain refinement, contributing to a remarkable 33% increase in the microhardness of the synthesized composite. In another investigation, Mashinini et al.[14] determined the optimal Friction Stir Welding (FSW) parameters for Ti-6Al-V. They identified a traverse speed of 40 mm min^{-1} as the most effective, with the maximum temperature reaching 980 °C. Interestingly, an increase in traverse speed from 40 to 200 mm min^{-1} resulted in a decrease in the ultimate tensile strength (UTS) of the samples from 1040 to 716 MPa. Jiang et al.[15] reported that titanium exhibited superior corrosion resistance with a hydroxyapatite (HA) coating. Additionally, they observed an improvement in cell adhesion on samples with HA coating.
Ultrafine-grained zones were achieved by Khodabakhshi et al. [16]through the FSP technique, yielding grains with a mean size of less than 1.4 µm. They established a correlation between the adsorption of nitrogen (N) and oxygen (O) elements and the presence of smaller grains. Temperature monitoring during the study revealed the transformation of titanium from a stable (α) to a

metastable (β) phase within the stir zone during the FSP process. In another study by Rahmati et al. [17], a surface layer with a mean hardness of 400 HV was obtained on the samples during FSP. The underlying layers exhibited hardness values around 250 HV, while the hardness of the titanium substrate was measured at 150 HV. Notably, they concluded that negatively affected tensile strength due to the formation of weak bonds with the titanium particles.
To the best of our knowledge, there are few studies focused on fabrication of HA-Ti surface composites via the FSP method [18]. However, a notable gap persists in understanding the impact of processing parameters i.e., filler content on the mechanical properties of HA-Ti surface composites. Therefore, this study addresses this gap by examining the mechanical behavior of FSPed HA-Ti composite coatings on Ti substrates. The research seeks to assess the influence of two different pastes on the mechanical properties of these surface composites.

2. Materials and Methods

2.1. Raw Materials

Commercially pure titanium sheet was prepared (Iran), with dimensions of 300 x 200 x 100 mm3. The elemental analysis of the titanium sheet was measured using optical emission spectrometer (OES), and the details are presented in Table. 1. The titanium plates underwent polishing to eliminate impurities and oxide layers. Subsequently, the plates were thoroughly rinsed in a solution consisting of ethanol and acetone in a 1:1 ratio. The hydroxyapatite powder was obtained from Sigma Aldrich company, (< 200 nm and purity of 99.9%). As illustrated in Fig. 1., the mean size of the HA powder is less than 50 nm.

2.2. Friction Stir Processing (FSP)

In the initial phase, the processing tool was meticulously designed with a shoulder diameter of 200 mm. One side of the tool was left without a pin for the capping step, while the other side was precisely machined into conical shape. The pin featured a minor diameter of 5 mm at the end, with the major diameter designed to be 6 mm adjacent to the shoulder. The pin height was consistently set at 4 mm. Tungsten carbide was chosen as the material for the tool due to its ability to withstand high working temperatures and the severe shear stress inherent in the FSP process.
Grooves with a depth of 3.5 mm and a width of 1.5 mm, were created lengthwise along the Ti sheet. The grooves were then washed and cleaned. Pastes of HA/acetone and HA/PVA were prepared followed by filling in the grooves using a spatula (Table. 2). To prevent the HA powder from dispersion during the FSP process, the top surface of the groove was covered with the pin-less tool. Subsequently, the primary FSP process for all samples was performed in three passes continuously, along the groove. The key parameters for the FSP process included a rotational speed of 1200 rpm, a traverse speed of 30 and 45 mm min-1, a tool penetration angle of 3° in respect to the normal axis, and a plunge depth of 0.5 mm.

Table. 2. FSPed samples used in this research.

No.	Sample	Filler	Traverse speed (mm min^{-1})
1	A30-HA-Ti	HA/acetone paste	30
2	A45-HA-Ti	HA/acetone paste	45
3	P30-HA-Ti	HA/PVA paste	30
4	P45-HA-Ti	HA/PVA paste	45

Table. 1. Chemical composition of the Ti sheet used in this research.

Element	Al	V	Cr	Fe	Mn	Mo	Nb	Sn	Ni	Ti
Composition(wt. %)	< 0.005	< 0.010	< 0.005	0.020	0.005	< 0.010	0.010	< 0.020	< 0.005	Base

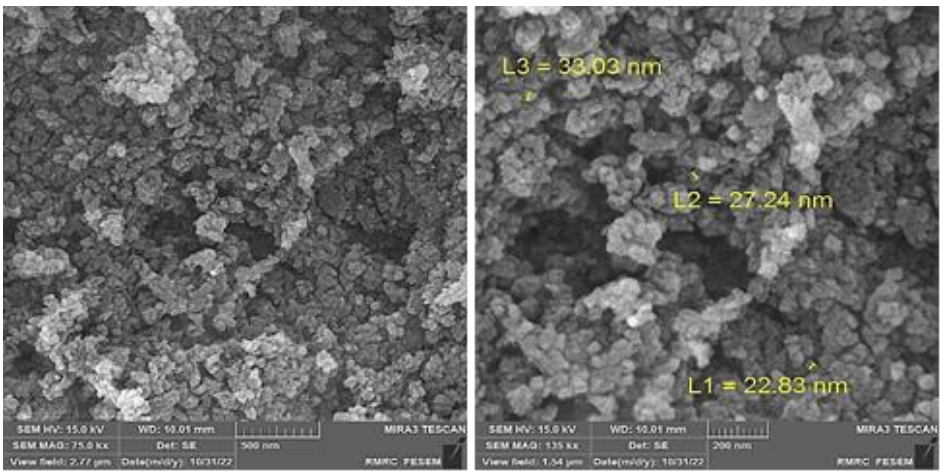

Fig. 1. The microstructure of the HA powder.

2.3. Macro/Micro Characterization of the Sample

To assess the microstructure, the sample was cut perpendicular to the traverse direction using electrical discharge machining (EDM). Following cutting, standard metallographic procedures were employed. Subsequently, the samples were polished and etched using Keller's reagent as detailed elsewhere [17]. Microstructural analysis was conducted using an Olympus GX41 optical microscope.
The grain size and microstructure, such as the Stir Zone (SZ), Heat-Affected Zone (HAZ), and Base Metal (BM), Thermo-Mechanically Affected Zone (TMAZ) formed during the FSP process, were evaluated through microscopic examination. For studying the distribution of HA powder on the fracture's surface, the samples were examined using a FESEM microscope (Mira II TESCAN) with the assistance of an EDS analysis.

2.4. Tensile Test

Tensile test was carried out in accordance with ASTM standard E8M (ASTM-E8/E8M-15, 2015), employing dog bone-shaped samples. The dimensions of the samples, including width and length, adhered to the sub-size dimensions outlined in ASTM E8. The prepared tensile specimens underwent testing using the SANTAM universal tensile testing machine (STM 25T, Iran) with a loading capacity of 25 KN. The tests were conducted at a crosshead speed of 5 mm min-1. To ensure result accuracy, each sample underwent three tests, and the reported result represents the average of the three obtained Ultimate Tensile Strength (UTS) values. Subsequently, the fractured samples were subjected to FESEM analysis.

2.5. XRD Analysis

To analyze the obtained phases, XRD analysis was employed using Cu Kα radiation. The analysis was conducted in continuous scanning mode at a rate of 1.8 o/min., in the range of 20 – 80o on an XRD Philips PW1730. The voltage and anode current used were 42 KV and 35 mA, respectively.
The phases were identified using PANalyticalHighScore Plus software V. 3.0.5.

3. Results and Discussion

3.1. Macro/Microstructure analysis

Fig. 2. shows the surface of the FSPed samples with traverse speeds of 30 mm min-1. It is clear that all samples show a good quality of surface. This implies that the FSP process is well performed and the HA paste is probably well dispersed into the Ti base metal. Thus, it can be said that the provided input heat for preparing the samples and filling the hole was adequate that is stated elsewhere (16).

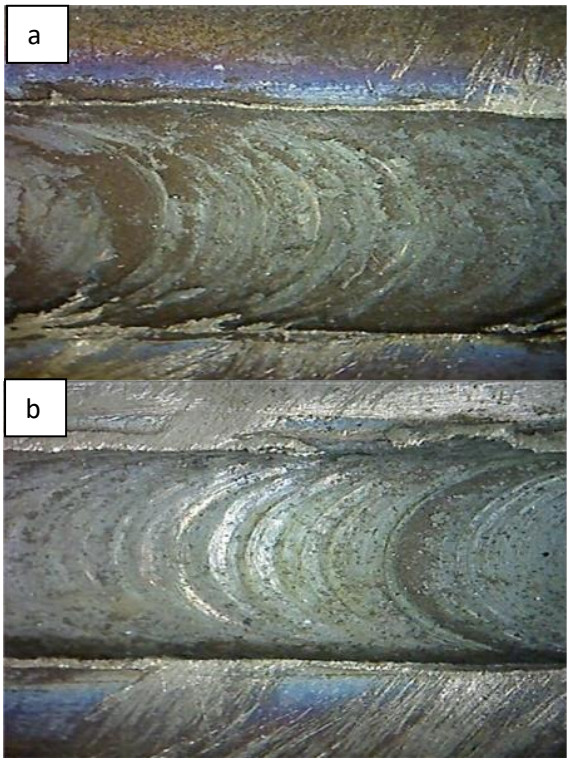

Fig. 2. The macrostructure surface of the FSPed (a) A30-HA-Ti and (b) P30-HA-Ti samples.

In order to further investigate the formation of possible defects in the samples, optical microscope images were provided (Fig. 3.). It is depicted that the Stirred Zone is lighter than other areas. It is clear that P30-HA-Ti and P45-HA-Ti samples have bigger SZ which is related to the prepared heat input during FSP as well as better fluidity of HA and PVA mixture [19].According to Fig. 3., there are two darker areas in A30-HA-Ti and A45-HA-Ti samples that require to be further investigated, since they can be signs of crack and porosities formation as well as inappropriate material flow during FSP.

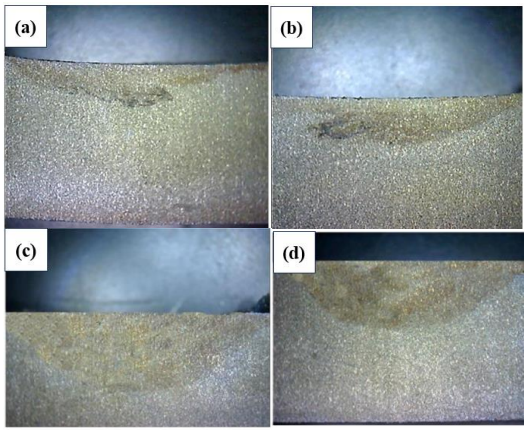

Fig. 3. Optical microscope images of the samples (a) A30-HA-Ti, (b) A45-HA-Ti, (c) P30-HA-Ti, and (d) P45-HA-Ti

The microstructure of the samples was further investigated by FESEM analysis. The micrographs of the samples are depicted in Fig. 4. It can be seen that there are some microcracks and porosities in the A30-HA-Ti and A45-HA-Ti samples. This can be attributed to the inappropriate trap of the HA powder in the Ti during FSP process. It should be noted that the presence of these microcracks would lead to lower tensile strength of the specimens. Also, it is evident that HA is well incorporated and dispersed in the P30-HA-Ti, and P45-HA-Ti specimens, confirming the positive effect of PVA as a surfactant for HA powder.

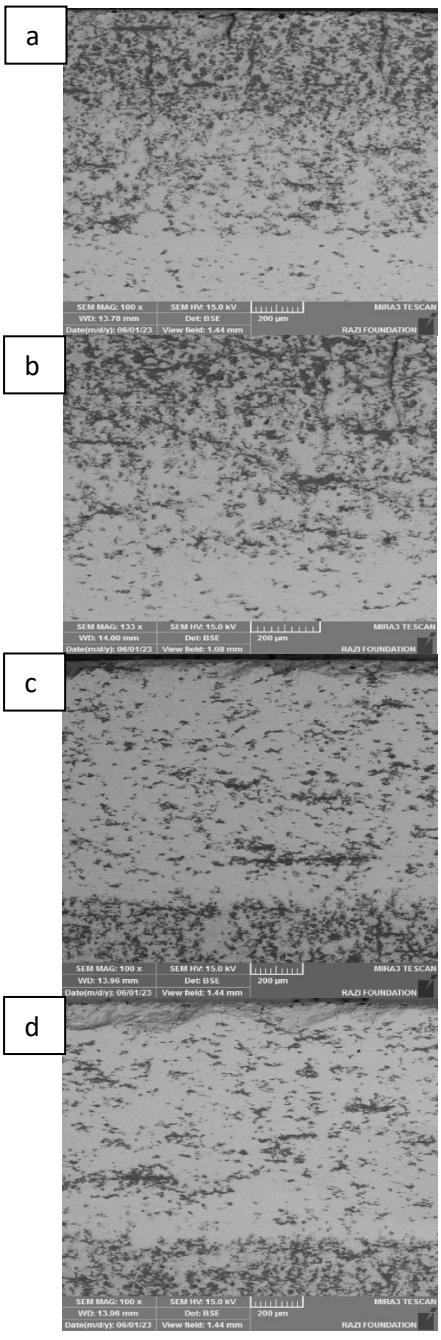

Fig. 4. Backscattered electrons FESEM images of the cross-section of FSPed (a) A30-HA-Ti, (b) A45-HA-Ti, (c) P30-HA-Ti, and (d) P45-HA-Ti samples.

Fig. 5. illustrates the EDS results obtained for A45-HA-Ti and P45-HA-Ti specimens. It is clear that there are agglomerates of HA in the sample FSPed with HA/acetone paste. This implies that acetone cannot act as a good surfactant for HA powder. This leads to inappropriate dispersion of the HA powder in the Ti base metal.

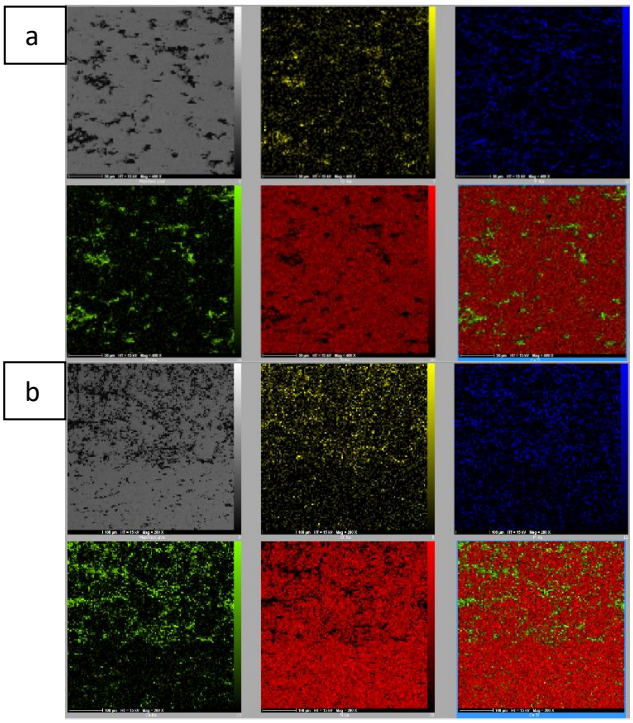

Fig. 5. EDS map analysis from the top surface of the (a) A45-HA-Ti and (b) P45-HA-Ti specimens

3.2. XRD Analysis

In order to investigate the obtained phases in the samples, XRD analysis was performed (Fig. 6). It can be seen that there exist small peaks of HA phase in all samples.

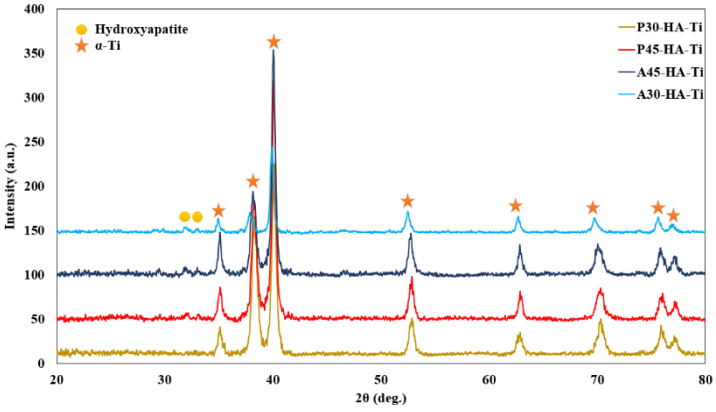

Fig. 6. XRD patterns of (a) A30-HA-Ti, (b) A45-HA-Ti, (c) P30-HA-Ti, and (d) P45-HA-Ti samples.

It is reported that Ti has higher mass attenuation coefficient (208 cm2 g-1) than that of HA (87

cm2/g-1) [20]. Therefore, the Ti matrix absorbs a considerable portion of the diffracted X-rays from the HA phase. This absorption contributes to the reduced intensity of the HA peaks.

It is evident that the prominence of the HA peaks increases with higher traverse speeds from 30 to 45 mm min-1. This variation in intensity can be ascribed to the altered distribution of phases on the sample's surface induced by the traverse speed. The higher traverse speeds may have led to the migration of the HA phase towards the composite surface, consequently enhancing the intensity of the associated peaks in the XRD pattern.

Furthermore, it is evident that the samples of A30-HA-Ti and A45-HA-Ti show more intense HA in the XRD patterns than that of P30-HA-Ti, and (d) P45-HA-Ti samples. This could be due the non-incorporation of HA particles into Ti base metal, that results in existence of more contents of HA in the surface of the HA-Ti surface composite. Also, agglomeration of HA in the A30-HA-Ti and A45-HA-Ti samples can be the reason of higher intensity of the HA peaks in the samples FSPed with HA/acetone paste. This is in good accordance with EDS results (Fig. 5.).

3.3. Tensile Test

The plots of the stress-strain for A30-HA-Ti, A45-HA-Ti, P30-HA-Ti, and P45-HA-Ti samples are depicted in Fig. 7. According to the plots, the measured values for ultimate tensile strengths of FSPed samples of A30-HA-Ti, A45-HA-Ti, P30-HA-Ti, and P45-HA-Ti were approximately 757 ± 26 MPa, 628 ± 16 MPa, 896 ± 28 MPa, and 763 ± 24 MPa, respectively.

It can be seen that samples FSPed with HA/PVA paste have higher ultimate tensile strength in both traverse speeds than that of samples FSPed with HA/acetone paste. This phenomenon can be due to agglomeration of HA powder during FSP process. This implies that PVA could act as a good surfactant for HA that leads to better dispersion of HA in the Ti base metal. This result is in good accordance with XRD and FESEM results.

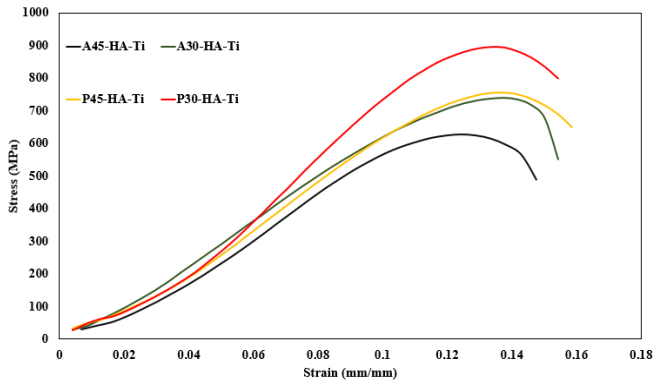

Fig. 7. Stress-strain plots of FSPed A30-HA-Ti, A45-HA-Ti, P30-HA-Ti, and P45-HA-Ti specimens.

4.Conclusion

In this study, HA-Ti surface composites were produced through FSP method. In order to investigate the effect of filler mixture, two different pastes of HA/acetone and HA/PVA were utilized for the FSP process in two traverse speeds of 30 and 45 mm min-1. The findings showed that the both pastes were incorporated in the Ti base metal. A heterogeneous and agglomerated distribution of HA particles was obtained in the Ti matrix when using HA/acetone paste for the FSP process .

From the comparison of the obtained results, it can conclude that:

1.Both pastes were incorporated in the Ti base metal.

2.Heterogeneous and agglomerated distribution of HA particles observed in Ti matrix with HA/acetone paste.

3.PVA acted as a surfactant for HA powder, resulting in better dispersion of hydroxyapatite particles in the titanium matrix.

4.Comparison of results showed that higher traverse speed led to lower mechanical properties.

5.Samples FSPed at 30 mm min-1 showed significantly higher mechanical properties with both HA/acetone and HA/PVA paste.

6.Higher mechanical properties, specifically tensile strength, observed in samples FSPed with HA/PVA paste.

7.The FSPed sample with HA/PVA paste, conical pin, rotational speed of 1200 rpm, and traverse speed of 30 mm min-1 acted as the best specimen in terms of mechanical properties.

References

[1] Sharma V, Prakash U, Kumar BM. Surface composites by friction stir processing: A Rev. J. Mater. Process. Technol. 2015; 224:117-34.

[2] Paidar M, Ghavamian S, Ojo OO, Khorram A, Shahbaz A. Modified friction stir clinching of dissimilar AA2024-T3 to AA7075-T6: effect of tool rotational speed and penetration depth. J. Manuf. Process. 2019; 47:157-71.

[3] Arres M, Salama M, Rechena D, Paradiso P, Reis L, Alves MM, do Rego AM, Carmezim MJ, Vaz MF, Deus AM, Santos C. Surface and mechanical properties of a nanostructured citrate hydroxyapatite coating on pure titanium. J. Mech.Behav. Biomed. Mater. 2020; 108:103794.

[4] Xu W, Hu W, Li M. Sol–gel derived hydroxyapatite/titania biocoatings on titanium substrate. Mater. Lett. 2006; 60(13-14):1575-8.

[5] Shafiei-Zarghani A, Kashani-Bozorg SF, Gerlich AP. Texture analyses of Ti/Al_2O_3 nanocomposite produced using friction stir processing. Metall Mater. Trans. A. 2016; 47:5618-29.

[6] Shafiei-Zarghani A, Kashani-Bozorg SF, Gerlich AP. Strengthening analyses and mechanical

assessment of Ti/Al_2O_3 nano-composites produced by friction stir processing. Mater. Sci. Eng. A. 2015; 631:75-85.
[7] Shamsipur A, Kashani-Bozorg SF, Zarei-Hanzaki A. The effects of friction-stir process parameters on the fabrication of Ti/SiC nano-composite surface layer. Surf. Coat. Technol. 2011; 206(6):1372-81.
[8] Shamsipur A, Kashani-Bozorg SF, Zarei-Hanzaki A. Production of in-situ hard Ti/TiN composite surface layers on CP-Ti using reactive friction stir processing under nitrogen environment. Surf. Coat. Technol. 2013; 218:62-70.
[9] Shamsipur A, Kashani-Bozorg S-F, Zarei-Hanzaki A. Surface Modification of Titanium by Producing Ti/TiN Surface Composite Layers via FSP. ACTA METALL SIN-ENGL. 2017; 30(6):550-7.
[10] Li B, Shen Y, Luo L, Hu W. Fabrication of TiCp/Ti–6Al–4V surface composite via friction stir processing (FSP): Process optimization, particle dispersion-refinement behavior and hardening mechanism. J. Mater. Sci. Eng A. 2013; 574:75-85.
[11] Ding Z, Zhang C, Xie L, Zhang L-C, Wang L, Lu W. Effects of Friction Stir Processing on the Phase Transformation and Microstructure of TiO2-Compounded Ti-6Al-4V Alloy. Metall. Mater. Trans. A. 2016; 47(12):5675-9.
[12] Hakakzadeh M, Jafarian HR, Seyedein SH, Eivani AR, Park N, Heidarzadeh A. Production of Ti-CNTs surface nanocomposites for biomedical applications by friction stir processing: Microstructure and mechanical properties. Mater. Lett. 2021; 300:130138.
[13] Farnoush H, Sadeghi A, Abdi Bastami A, Moztarzadeh F, Aghazadeh Mohandesi J. An innovative fabrication of nano-HA coatings on Ti-CaP nanocomposite layer using a combination of friction stir processing and electrophoretic deposition. Ceram. Int. 2013; 39(2):1477-83.
[14] Mashinini PM, Dinaharan I, David Raja Selvam J, Hattingh DG. Microstructure evolution and mechanical characterization of friction stir welded titanium alloy Ti–6Al–4V using lanthanated tungsten tool. Mater Charact. 2018; 139:328-36.
[15] Jiang J, Han G, Zheng X, Chen G, Zhu P. Characterization and biocompatibility study of hydroxyapatite coating on the surface of titanium alloy. Surf. Coat. Technol. 2019; 375:645-51.
[16] Khodabakhshi F, Rahmati R, Nosko M, Orovčík L, Nagy Š, Gerlich AP. Orientation structural mapping and textural characterization of a CP-Ti/HA surface nanocomposite produced by friction-stir processing. Surf. Coat. Technol. 2019; 374:460-75.
[17] Rahmati R, Khodabakhshi F. Microstructural evolution and mechanical properties of a friction-stir processed Ti-hydroxyapatite (HA) nanocomposite. J. Mech.Behav. Biomed. Mater. 2018; 88:127-39.
[18] Shahbaz A, Abbasi M, Sabet H. Effect of microstructure on mechanical, electrochemical, and biological properties of Ti/HA surface composites fabricated by FSP method. Mater. Today Commun. 2023; 37:107305.
[19] Abdi Bastami A, Farnoush H, Sadeghi A, Aghazadeh Mohandesi J. Sol–gel derived nanohydroxyapatite film on friction stir processed Ti–6Al–4V substrate. Surf. Eng. 2013; 29(3):205-10.
[20] Jenkins R, Snyder RL. Introduction to X-ray Powder Diffractometry (Volume 138): Wiley Online Library; 1996.